jmr&t
Journal of Materials Research and Technology
www.jmrt.com.br

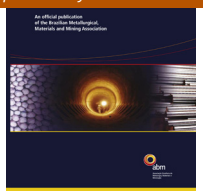

Review Article

Microstructural evaluation of an asymmetrically rolled and recrystallized 3105 aluminum alloy

Saulo Brinco Diniz[a,*], *Emanuel Alejandro Benatti*[b], *Andersan dos Santos Paula*[a,c], *Raúl Eduardo Bolmaro*[b], *Luis Celso da Silva*[d], *Bruna Godoi Meirelles*[e]

[a] *Instituto Militar de Engenharia (IME), Rio de Janeiro, RJ, Brazil*
[b] *Facultad de Ciencias Exactas, Ingeniería y Agrimensura, Universidad Nacional de Rosario (UNR), Provincia de Santa Fe, Argentina*
[c] *Post-Graduate Program in Metallurgical Engineering, Universidade Federal Fluminense (UFF), Volta Redonda, RJ, Brazil*
[d] *Escola de Engenharia Industrial e Metalúrgica de Volta Redonda (EEIMVR), Universidade Federal Fluminense (UFF), Volta Redonda, RJ, Brazil*
[e] *Votorantim Metais, Alumínio, SP, Brazil*

ARTICLE INFO

Article history:
Received 27 April 2014
Accepted 17 February 2016
Available online 3 April 2016

Keywords:
Aluminum alloy
Asymmetric rolling
Superplasticity
Solubilization heat treatment

ABSTRACT

This study evaluates the influence of the structural changes promoted by a solution heat treatment (ST) on recrystallization and grain growth during annealing of the 3105 Al alloy subject to asymmetric rolling. Optical Microscopy, Scanning Electron Microscopy (SEM)/X-Ray Energy Dispersive Spectroscopy (EDS), X-Ray Diffraction (XRD), dilatometric analysis and Vickers hardness tests were used to evaluate the microstructural and mechanical properties. The influence of solution heat treatment on grain growth kinetics could not be evaluated because of incomplete recrystallization due to the chosen annealing parameters.

1. Introduction

According to the present scenario, searching for greater energy efficiency and weight reduction of metallic structures in aeronautical and automotive industries is a valuable strategy. This weight reduction has been achieved, for example, through the elimination of joining processes, such as welding and riveting. The conformation of parts with complex geometries is an excellent choice to avoid joining, and superplasticity, obtained through materials with ultrafine grains [1,2], has gained interest over the last few years as a mean of achieving deformation of complex shapes. A techniques called Severe Plastic Deformation (SPD) was created and is considered a viable alternative to obtain materials with ultrafine grain size [3–5].

To achieve the superplasticity property in metals, it is not only necessary to obtain ultrafine grain size, but also equiaxed recrystallized grains with high angle disorientation and precipitates or second phase particles [1,6]. This last characteristic is very important for superplasticity, because the materials processed by SPD techniques, in order to exhibit

* *Corresponding author.*
E-mail: sbdinniz@outlook.com (S.B. Diniz).
http://dx.doi.org/10.1016/j.jmrt.2016.02.001

superplastic behavior, experience high temperatures in various steps of the process, during which, without the presence of these second phase particles, grain growth would occur, and superplasticity would be spoiled.

Thus, alloys having coarse precipitates, such as most alloys produced at industrial scale, that do not require a rigorous control of these particles, are not suited for the superplasticity applications, because according to Gottstein [7], a particle size less than 50 nm is needed to avoid the grain growth.

In order to provide a convenient microstructure, including precipitate size, to enable superplastic behavior on some metals where the solute concentration is slightly above the solubility limit of the solvent, e.g. aluminum and aluminum alloys, a heat treatment is an effective option, providing size reduction of coarse precipitates and complete dissolution of some others.

In the broadest sense, this heat treatment consists of heating an alloy at a sufficiently high temperature for a time long enough to achieve a nearly homogeneous solid solution in which almost all solutes are dissolved, so that a single-phase structure is attained [8,9].

This study evaluated the influence of a solution heat treatment (ST), on retardation of the recrystallization and/or retention of grain growth when a 3105 aluminum alloy is subject to asymmetric rolling and recrystallization for different soaking times. This alloy is commonly used in simple applications where size control of the second phase particles is not necessary, but has the potential to improve the mechanical properties of the alloy.

2. Material and methods

2.1. Material

The material used for this study was a 3105 aluminum alloy, a 7 mm thickness hot-rolled sheet, donated by Votorantim Metals (originally from Aluminum/SP, Brazil). Table 1 shows the sheet chemical composition.

Sample nomenclature is as follows:

(i) The leading four digits represent the alloy analyzed = 3105;
(ii) The following two letters indicate the initial condition of the alloy: AR = As Received and ST = subject to a Solution heat Treatment;
(iii) The last two symbols indicate the final condition of the sample processing: AS = ASymmetrically rolled or 15, 30, 45 or 60 = asymmetrically rolled and subject to an annealing heat treatment for recrystallization with soaking times of 15, 30, 45 and 60 min, respectively.

2.2. Methods

Half of the samples were subject to ST in an electric resistance furnace at a soaking temperature of approximately 500 °C for 60 min, and where quenched in water at room temperature under agitation.

For ASymmetric rolling (AS), was used a pilot-mill with the rolling cylinders revolving at the same speed (1.676 rad/s), in the same direction and with the same coefficient of friction and a ratio between cylinder radii ~ 1.18. The rolling directions of the AR sheet and the AS process are the same. These tests were conducted at room temperature, after 90 passes with a thickness reduction of about 4.7% per pass.

After the AS, small samples with dimensions of approximately 2 × 20 × 10 mm were cut and subjected to Annealing Heat Treatment for Recrystallization (AHTR) at a soaking temperature of 350 °C with 4 distinct soaking times (15, 30, 45 and 60 min) and then cooled in air.

For the microstructure characterization, the samples were cut and metallographically prepared according to the following procedures:

- for Vickers hardness measurements and Scanning Electron Microscopy (SEM)/X-Ray Energy Dispersive Spectroscopy (EDS), the samples were hot encapsulated with phenolic resin, sanded with 220–4000 mesh SiC paper and mechanically polished with diamond pastes (6 μm, 3 μm and 1 μm).
- for Vickers hardness measurements in the AS samples subject to AHTR with different soaking times, the samples were cold encapsulated with acrylic resin instead, before being subject to the same grinding and polishing procedure.
- for X-Ray Diffraction (XRD) and optical microscopy, the samples (not encapsulated) were subject to the same sanding step (sandpaper with grain size 220–4000 mesh) followed by electrolytic polishing (solution: 59% CH_4O, 35% $C_2H_4(OH)_2$ and 6% $HClO_4$ (in volume); electric potential difference between 14 and 24 V during 10–24 s at room temperature).

The microstructure observation by Optical Microscope – OM (Image Pro Plus software) was performed over points associated with ¼ and ½ in thickness cross section associated to the rolling direction (RD).

The SEM analysis was performed with the secondary electron detector: 12 keV, spot size of 500 and a working distance of 11 mm.

The Vickers hardness test (Manufacturer Spectrum Instrumental Scientific LTD) was performed with a load of 100 g (0.1 kgf) and a dwelling time of 18 s. For samples on AR and ST conditions, 10 measurements were performed, at ½ and ¼ of the thickness, and at ¼, ½ and ¾ of the thickness for the samples processed by AS.

Table 1 – Aluminum 3105 alloy – chemical composition (weight percent).

	Chemical composition (%)									
	Si	Fe	Cu	Mn	Mg	Ti	Cr	Zn	Other	Al
3105 alloy	0.220	0.540	0.094	0.580	0.580	0.020	0.011	0.036	0.025	Remainder

The dilatometric tests were conducted on a thermo-mechanical analyzer (TMA); the samples had approximate dimensions of $5 \times 5 \times 2$ mm. The sample faces were sanded with silicon carbide sandpaper (320–4000 mesh), and chemically polished in an acid solution (50% HNO_3 and 50% HF) for 10 min. In the TMA furnace, the samples were heated from room temperature to 350 °C (heating rate 8 °C/min) soaked for 60 min and cooled in air.

The X-ray diffraction analysis was performed with a Shimadzu diffractometer (XRD-6000) with Co-Kα radiation, standard goniometer, 30 kV, 30 mA, $\theta/2\theta$ coupling scans in the range of 20° to 110° for 2θ, with 2θ step of 0.02° and speed of 2°/min. The relative intensity (%) and half width of the measured peaks from the XRD spectra were analyzed with the assistance of the "Spectroscopy/Baseline and Peaks" function available at "Origin Pro 8" software.

3. Results and discussion

3.1. *Characterization of starting material – AR and ST condition comparison*

The samples on AR and ST conditions were observed over the regions at ¼ and ½ thickness. Fig. 1 shows the microstructures observed by optical microscope (OM) of the 3105 alloy on AR (Fig. 1(a) and (b)) and ST (Fig. 1(c) and (d)) conditions, both observed at ¼ and ½ of the thickness, with a magnification of 200×.

Fig. 1 shows two circles marked with "1" and "2", two distinct morphologies of coarse precipitates. At ½ thickness, we can observe the presence of two distinct types: (a) precipitates indicated by "1" have an apparently elongated/needle shape (thin precipitates), (b) precipitates indicated by "2" shows an apparently lamellar shape (coarse precipitate). These two distinct precipitate shapes are not found when observing ¼ of thickness regions. Fig. 1(c) and (d) only show precipitates characterized as elongated/needle shape (thin precipitates) indicated by "1". These quite distinct precipitate shapes may be associated with the difference in segregation of solute across the thickness during solidification produced after hot rolling.

Comparing the microstructures shown in Fig. 1, it can be seen a decrease in the volume fraction of the precipitates indicated by "2". It can also be observed after the ST for the 3105 alloy, that there is an apparent reduction in the volume fraction of elongated/needle shape precipitates (thin precipitates) indicated by "1", and, most likely, a complete dissolution of those precipitates.

Such microstructural characteristics obtained after the solution heat treatment (ST condition) revealed the reduction of the precipitate volumetric fraction (types 1 and 2). Thus, in materials the ST condition, there is possibly a better microstructural condition for the achievement of superplasticity than in materials in the AR condition, since the precipitates have an important role in the grain growth retention during exposure to high temperatures [10].

Fig. 2 shows the microstructure at ½ thickness regions for the 3105 alloy on AR and ST conditions, obtained by the secondary electrons and EDS detectors coupled to SEM. The main precipitates are indicated by numerical indices on the images, which are referenced by their chemical composition analysis measured with the EDS probe and listed in Table 2.

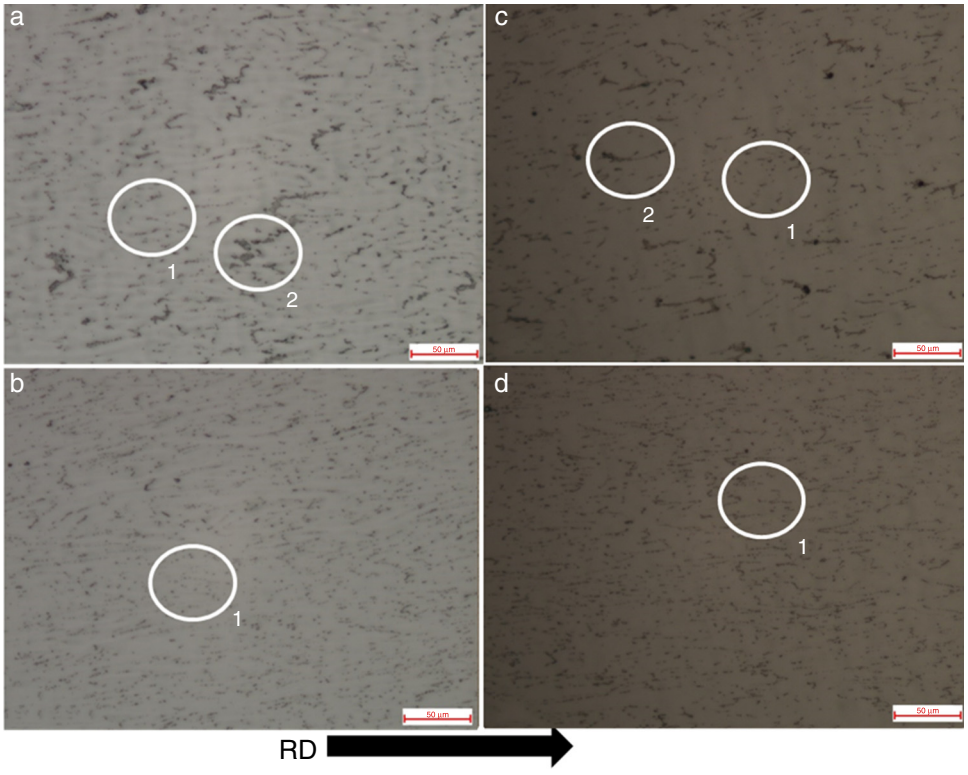

Fig. 1 – Microstructure of the 3105 alloy. (a) 3105-AR sample – ½ thickness, (b) 3105-AR sample – ¼ of thickness, (c) 3105-ST sample – ½ thickness, (d) 3105-ST sample – ¼ of thickness. Electrolytic Polishing, OM, 200×.

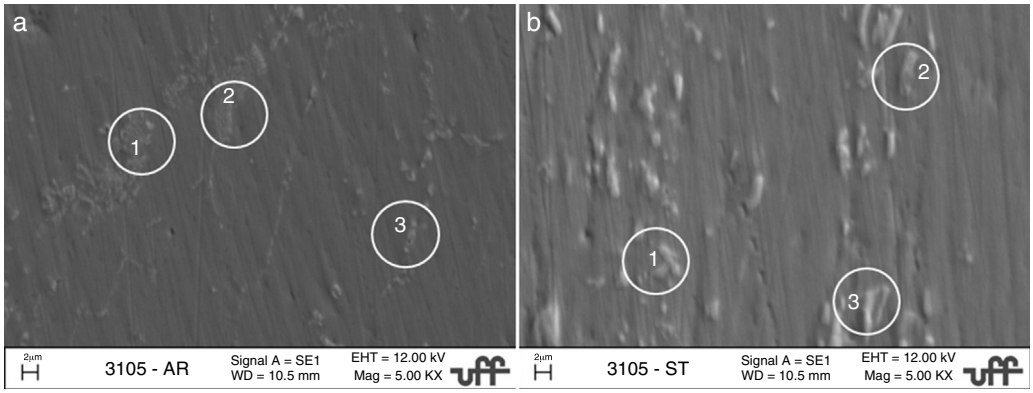

Fig. 2 – Microstructures on AR and ST condition of the 3105 alloy: (a) 3105-AR at ½ thickness; (b) 3105-ST at ½ thickness. Mechanical polishing. SEM, 5000×.

Table 2 – Chemical composition by EDS for 3105 alloy on AR and ST condition associated to distinct points, according to the indications in Fig. 3. Values in weight percent.

			Elements (%)				
			Fe	Cu	Mn	Al	O
3105-AR sample	½ thickness	Point 1	–	1.36	13.15	85.48	–
		Point 2	5.79	1.12	3.31	89.78	–
		Point 3	4.97	1.58	–	92.78	0.68
3105-ST sample	½ thickness	Point 1	19.87	–	5.16	74.97	–
		Point 2	3.94	–	–	96.06	–
		Point 3	13.78	–	5.7	80.52	–

In the microstructure observed by SEM (Fig. 2), it can be clearly seen that the precipitated shape changed from AR to ST. The sample 3105-AR (Fig. 2(a)) had precipitates in the interdendritic zone, which are due to solute segregation between α phase dendrites (rich in aluminum) that compose a eutectic morphology structure (precipitates and the α phase matrix). Moreover, the sample ST-3105 precipitates (Fig. 2(b)) have an almost spheroidal shape.

In the EDS results, the presence of large percentages of Al is due to the Al phase matrix surrounding the precipitate, especially for smaller precipitates, because of the large sampling volume implied by EDS technique. For a point analyzed on AR condition, oxygen was found, which is probably associated with oxides resulting from impurities.

According to the literature [11], addition of elements such as Si, Fe, Mn and Cu increases the hardness of aluminum alloys hardness. Comparing the chemical compositions of AR and ST samples (Table 2) it can be seen that there is a decrease in the weight percentage of these elements in the precipitates (points analyzed by EDS – Fig. 2). Because probably those elements partially constituted the precipitates contributing to their size, their reintroduction as solid solution in the matrix by partial dissolution during ST, is compensated by a decrease in precipitate size.

Fig. 3 shows a comparison between the hardness of the AR and ST conditions in relation to the positioning of hardness measurement.

As to hardness measurement positions (¼ and ½ of thickness), it can be seen that there were no significant differences. The standard deviations of the hardness measurements were small in regions at ¼ and ½ of thickness, this fact shows that the differences on precipitates sizes, shapes and compositions between ¼ and ½ of thickness (Fig. 1) were not enough to promote significant changes on mechanical properties, as measured through Vickers hardness (Fig. 3) either on AR or ST conditions.

Comparing the Vickers hardness measurements on AR to ST conditions (Fig. 3), it can be seen a decrease about of 18.8% on Vickers hardness from AR to ST conditions (Fig. 3), indicating a possible solute incorporation on the matrix by precipitate dissolution during ST. However, this change can also be associated with grain growth promoted by the temperature and soaking time during the ST.

Based on the comparison of the results obtained for the 3105 alloy on AR and ST conditions, it was concluded that the ST was effective.

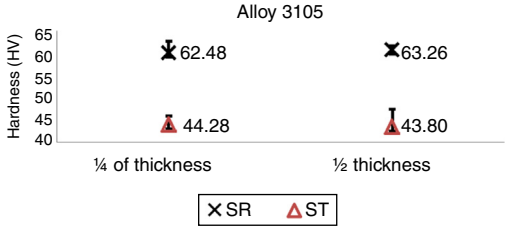

Fig. 3 – Comparison of hardness values (average and pattern deviation) of the 3105 alloy on AR and ST conditions at ¼ and ½ of thickness regions.

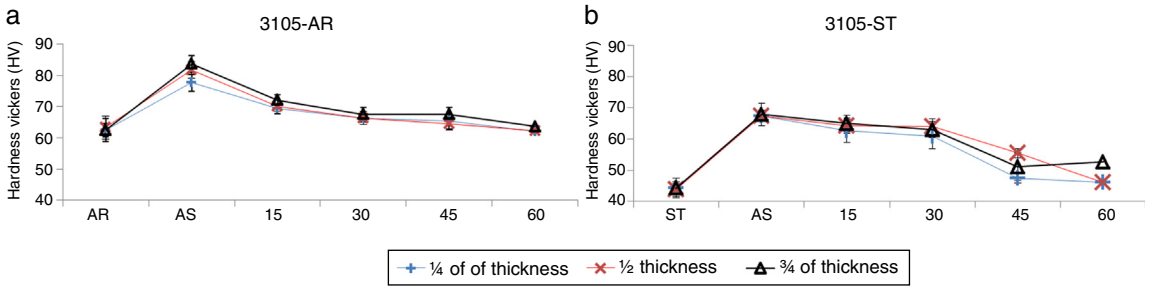

Fig. 4 – Vickers hardness evolution of 3105-AR and 3105-ST samples, after AHTR compared to AS and AR or ST previous conditions.

3.2. *Asymmetric rolling and annealing heat treatment for recrystallization*

Fig. 4 illustrates the 3105 alloy Vickers hardness evolution vs. recrystallization times. These samples were processed by ASymmetric rolling (indicated by AS) from the AR and ST previous conditions, and subsequently annealed for recrystallization at 350 °C with soaking times of 15, 30, 45 and 60 min.

The differences on Vickers hardness at ¼, ½ and ¾ of thickness are not very significant and perhaps only due to through thickness strain heterogeneity, and consequent grain sizes, because of rolling process characteristics [12–14]. The standard deviations of hardness measurements for 3105-AR-AS and 3105-ST-AS samples are a little larger than the standard deviations on the starting material (without processing by AS) although it is not very large and show an increase with increasing hardness.

As can be seen in Fig. 4, after processing by AS there was an increase in the 3105-AR and 3105-ST Vickers hardness due to strain hardening by grain refinement [15,16].

For the samples analyzed in different initial conditions, there is a small decrease in hardness between the AS condition (processed by Asymmetric Rolling) and "15" (AHTR with 15 min of soaking time) (Fig. 4). This decrease in hardness is associated with the onset of recrystallization during the first 15 min of soaking time.

Fig. 4 shows a tendency to decreasing hardness values for the recrystallized samples from the 3105-AR and 3105-ST conditions. This behavior indicates a non-hardness stabilization for longer times associated with the soaking times explored on this study to promoted recrystallization on AS samples, which possibly indicates that a maximum time of 60 min adopted in the AHTR may not have been sufficient to promote full recrystallization on strain-hardened structure.

Such incomplete recrystallization of 3105 alloy in AR or ST conditions might be due to the barriers created by precipitates that controlled the growing of the recrystallized regions [17]. Another factor that could explain the incomplete recrystallization of the samples in the 3105-AR and 3105-ST conditions could be the alloying element on solid solution, which possibly slows down recrystallization process at 350 °C.

Comparing the AR and ST conditions, it can be seen that the decrease of hardness, occurred mainly in the first 15 min for the AR condition, while, for the ST condition, the hardness decrease happened mainly in between 30 and 45 min.

Fig. 5 shows the dilatometry curve represented by the thickness variations as functions of temperature and soaking time, for the 3105-AR and 3105-ST samples processed by AS.

For the 3105-AR-AS and 3105-ST-AS samples (Fig. 5) the first inflections appeared at 43 °C and 42 °C, respectively, inflections probably associated to the beginning of the recovery process for these samples. The second inflections, which are probably associated with the recrystallization start for the samples, occur at temperatures of 180 °C and 250 °C, respectively.

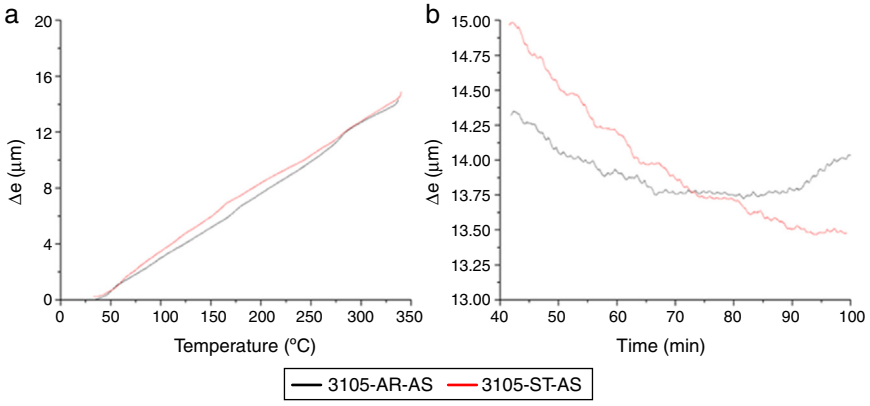

Fig. 5 – Dilatometry curves (a) thickness variation (Δ*e*) vs. temperature; (b) thickness variation (Δ*e*) vs. soaking time, for the samples 3105-AR-AS and 3105-ST-AS.

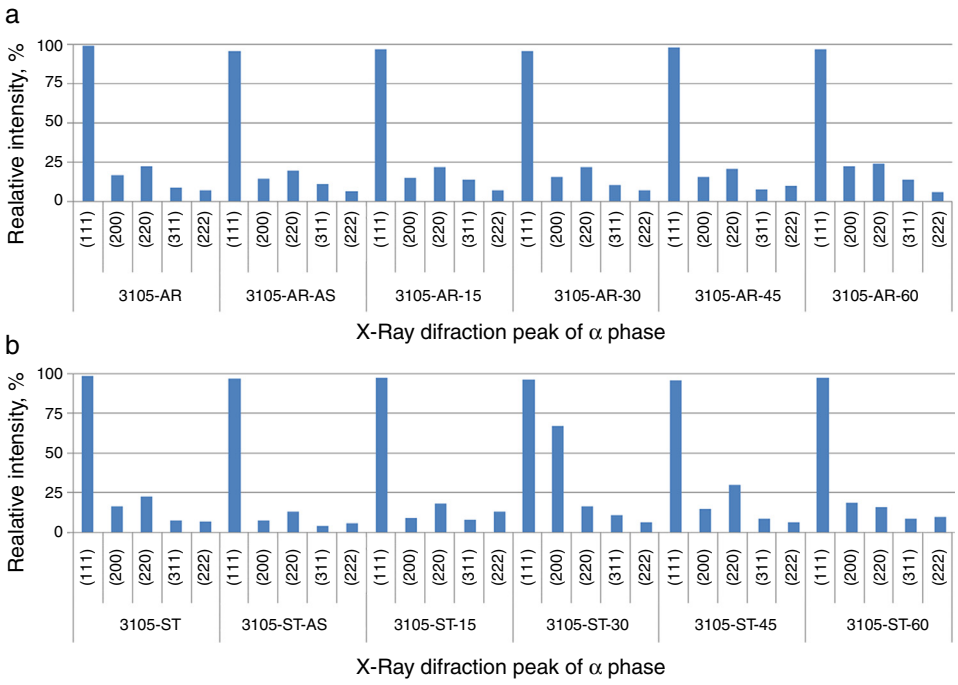

Fig. 6 – Effect of AHTR in the relative intensities (%) of the X-ray diffraction peaks for α phase in 3105 alloy: (a) AR previous condition, (b) ST previous condition.

In Fig. 5, slowly decreasing Δe values can be observed, but without a significant change in the curve inflection and with no stabilization of thickness variation, which was attributed to recrystallization progress on strain-hardened structures of the 3105-ST-AS and 3105-AR-AS samples. In the 3105-AR-AS sample there is a different behavior above 50 min of soaking time showing an increase in the Δ*e* values. These variations are not significant (less than 0.5 μm), and could be associated with probe movements, vibrations during the dilatometric analysis in the TMA and/or sample surface roughness.

Comparing Δ*e* (Fig. 5) with Vickers hardness evolution (Fig. 4(b)) vs. soaking time curves during the AHTR, a similar behavior can be observed for both 3105-AR-AS and 3105-ST-AS samples. There was a decrease on the hardness without reaching a constant value during heat treatment (Fig. 4); that can be associated with incomplete recrystallization of the strain-hardened structure promoted by AS process.

Fig. 6 shows the results of diffraction peak analysis, connected with structural evolution, for the AR and ST samples, after being processed by AS and further subject to AHTR.

Analyzing Fig. 6, it can be seen that there were not significant changes in the relative intensities of α phase diffraction peaks; the (111) diffraction peak has the highest intensity and (222) and (311) diffraction peaks has the lowest intensity, while the intermediate values of intensity take turns among the (200) and (220) peaks.

For the AR conditions, the "Relative Intensity (%)" results (Table 3) show an increase of the apparent volume fraction of (111) grain-oriented for the 3105-AR-AS to 3105-AR-15 condition, and 3105-AR-30 to 3105-AR-45 condition, and apparent decrease in the volume fraction for the 3105-AR-15 to 3105-AR-30 condition, and 3105-AR-45 to 3105-AR-60 condition. For the ST conditions, it can be inferred that there was an apparent increase of the volume fraction of (111) grain-oriented, of the 3105-ST-AS to 3105-AR-15 condition, and 3105-ST-45 to 3105-ST-60 condition, and apparent volume fraction decrease in the 3105-ST-15 to 3105-ST-45 condition.

The peak width can be associated with grain size and/or dislocation densities: a large peak width means smaller grains and/or larger dislocation densities. Thus, as can be seen by dilatometry (Fig. 5) and hardness tests (Fig. 4), there was not a total recrystallization and thus the "width at half height" cannot be associated with grain growth.

Table 3 – Effect of AHTR in the peak broadening for the (111)α diffraction plane for the 3105 alloy. (a) AR previous condition and (b) ST previous condition.

Sample	Relative intensity (%)	Width at half height
AR condition		
3105-AR	98.96	0.234
3105-AR-AS	95.52	0.222
3105-AR-15	96.93	0.186
3105-AR-30	95.92	0.159
3105-AR-45	98.04	0.182
3105-AR-60	96.71	0.178
ST condition		
3105-ST	98.53	0.198
3105-ST-AS	96.96	0.197
3105-ST-15	97.39	0.208
3105-ST-30	96.19	0.200
3105-ST-45	95.88	0.204
3105-ST-60	97.40	0.210

According to the "width at half height", for the AR conditions, can be inferred that there was a decrease in the dislocation densities for the 3105-AR-AS to 3105-AR-30 condition. This behavior may be associated with the recrystallization process, however, the increase in the dislocation densities for the 3105-AR-30 to 3105-AR-45 condition, may be associated with different levels of dislocations densities from one sample to another before the AHTR, in which even partly recrystallized may have a higher dislocations levels than the previous sample. For the 3105-AR-45 to 3105-AR-60 condition, there were not significant changes in the "width at half height" peak, the small difference may be associated with small errors in the XRD analysis. Therefore, it can be said that there was no change in the dislocation densities.

For the ST conditions, it can be inferred that there was a small increase in the dislocation densities in the 3105-ST-AS to 3105-ST-15 condition. This behavior can be explained in the same way as above, i.e., it can be attributed to different levels of dislocations densities from one sample to another before the AHTR. For the 3105-ST-15 to 3105-ST-60 condition, there were not significant changes in the "width at half height" peak, the small difference may be associated to small errors during XRD analysis and therefore it can be inferred that there was no change in the dislocation densities.

In general, according to the data presented, ST was able to provide a different structure than that observed on the AR condition.

4. Conclusion

The results of this work lead to the following conclusions:

I According to the results of Vickers hardness there is a structural homogeneity for the 3105 alloy through the thickness in both conditions, since when a comparison made in the ¼ and ½ thickness positions, there were no significant changes.

II In the analysis by Optical Microscopy (OM), it can be observed an apparent reduction in size and volume fraction of the precipitates after the solubilization heat treatment.

III According to the results of dilatometry analysis and Vickers hardness, it can be inferred that for the 3105 alloy (AR and ST conditions), there was not complete recrystallization for the maximum soaking time used in this study (60 min).

IV Based on the X-ray diffraction peak broadening, comparing the condition AR to ST, possibly the solubilization heat treatment may have caused a change in the microstructure during the annealing heat treatment for recrystallization.

V It was not possible to evaluate the effect of ST previous condition on retention of grain growth during the AHTR, due to the incomplete recrystallization on the AS samples, but the ST promoted a deceleration in the recrystallization, as can be seen from the values of Vickers hardness and dilatometric analysis.

Conflicts of interest

The authors declare no conflicts of interest.

Acknowledgments

The authors thank Votorantim Metals for providing the material used in for this study; CAPES for a Master and PhD scholarship (S. B. Diniz); Fundação Euclides Cunha (FEC), of Universidade Federal Fluminense (UFF), for the financial resources that contributed to a visit to Universidad Nacional de Rosario; Universidad Nacional de Rosario for the Asymmetric Rolling processing of the samples; and Multiuser Laboratory of Electronic Microscopy (LMME) of the Universidade Federal Fluminense for the use of their Scanning Electronic Microscope including sample preparation and data analysis.

REFERENCES

[1] Nieh TG, Wadsworth J, Shelby OD. Superplasticity in metals and ceramics. New York: Cambridge University Press; 2005.
[2] Furukawa M, Horita Z, Nemoto M, Langdon TG. Achieving superplasticity at high strain rates using equal channel angular pressing. Mater Sci Technol 2000;16:1330–3.
[3] Segal VM. Materials processing by simple shear. Mater Sci Eng A 1995;197:157–64.
[4] Santos MO [MSc dissertation] Processamento do Cobre por EACI. Brazil: Universidade Federal de Minas Gerais; 2008.
[5] Calado WR [DSc dissertation] Ultra-Refino de Grão Através de Deformação Plástica Severa por Ensaios de Torção: Simulação do Processo ARB. Brazil: Universidade Federal de Mimas Gerais; 2012.
[6] Xu C, Furukawa M, Horita Z, Langdon TG. Using ECAP to achieve grain refinement, precipitate fragmentation and high strain rate superplasticity in a spraycast aluminum alloy. Acta Mater 2003;51:6139–49.
[7] Gottstein G, Shvindlerman LS. On the retardation of grain boundary motion by small particles. Scripta Mater 2010;63:1089–91.
[8] ASM International. ASM handbook, heat treating; 1991.
[9] Monteiro VM, Diniz SB, Meirelles BG, Silva LC, Paula AS. Microstructural and mechanical study of aluminium alloys submitted to distinct soaking times during solution heat treatment. Tecnol Metal Mater Miner São Paulo 2014;11(4):1–8.
[10] Porter DA, Easterling K. Phase transformations in metals and alloys. 2nd ed. New York: Editora Chapman and Hall; 1992, 454f. Volume Único.
[11] ASM International. ASM handbook, properties and selection: nonferrous alloys and special-purpose materials; 1990.
[12] Ji HY, Park JJ. Development of severe plastic deformation by various asymmetric rolling processes. Mater Sci Eng 2009;499:14–7.
[13] Lee JK, Lee DN. Texture control and grain refinement of AA1050 Al alloy sheets by asymmetric rolling. Int J Mech Sci 2008;50:869–87.
[14] Zuo FQ, Jiang JH, Shan AD, Fang JM, Zhang XY. Shear deformation and grain refinement in pure Al by asymmetric rolling. Trans Nonferr Metals Soc China 2008;18:774–7.
[15] Meyers MA, Chawla KK. Princípios de Metalurgia Mecânica. São Paulo: Editora Edgar Blucher LTDA; 1982.
[16] Minatel R [MSc dissertation] Um Estudo Comparativo Sobre a Recristalização de Chapas de Alumínio AA1200 e AA3003 Obtidas por Lingotamento Contínuo (Twin RollCaster) e por Fundição de Placas (Direct Chill). Brazil: Universidade de São Paulo; 2009.
[17] Humphreys FJ, Hatherly M. Recrystallization and relates annealing phenomena. 2nd ed. Oxford: Elsevier LDT; 2004.